Developing Biohybrid Robotic Jellyfish (*Aurelia aurita*) for Free-swimming Tests in the Laboratory and in the Field

Nicole W. Xu[1, 2, *], James P. Townsend[3, 4], John H. Costello[3, 4], Sean P. Colin[3, 5], Brad J. Gemmell[6], John O. Dabiri[2, 7]

[1]Department of Bioengineering, Stanford University, Stanford, CA, USA; [2]Graduate Aerospace Laboratories (GALCIT), California Institute of Technology, Pasadena, CA, USA; [3]Marine Biological Laboratory, Woods Hole, MA, USA; [4]Department of Biology, Providence College, Providence, RI, USA; [5]Department of Marine Biology and Environmental Science, Roger Williams University, Bristol, RI, USA; [6]Department of Integrative Biology, University of South Florida, Tampa, FL, USA; [7]Department of Mechanical Engineering, California Institute of Technology, Pasadena, CA, USA
*For correspondence: nicolexu@alumni.stanford.edu

[Abstract] Biohybrid robotics is a growing field that incorporates both live tissues and engineered materials to build robots that address current limitations in robots, including high power consumption and low damage tolerance. One approach is to use microelectronics to enhance whole organisms, which has previously been achieved to control the locomotion of insects. However, the robotic control of jellyfish swimming offers additional advantages, with the potential to become a new ocean monitoring tool in conjunction with existing technologies. Here, we delineate protocols to build a self-contained swim controller using commercially available microelectronics, embed the device into live jellyfish, and calculate vertical swimming speeds in both laboratory conditions and coastal waters. Using these methods, we previously demonstrated enhanced swimming speeds up to threefold, compared to natural jellyfish swimming, in laboratory and *in situ* experiments. These results offered insights into both designing low-power robots and probing the structure-function of basal organisms. Future iterations of these biohybrid robotic jellyfish could be used for practical applications in ocean monitoring.

Keywords: Jellyfish, *Aurelia aurita*, Robotics, Biohybrid robot, Swimming, Speed, Ocean monitoring

[Background] Despite the importance of the ocean and need to track its changing conditions, over 80% of the ocean remains largely unobserved and unexplored (Kim *et al.,* 2012; Malve, 2016; NOAA, 2020a and 2020b). Further exploration is fundamental to reveal physical and biogeochemical processes in the ocean. This can improve our understanding of climate change, as well as provide new sources of food, medicine, and energy (NOAA, 2020b).

Traditional methods for ocean monitoring and exploration include remotely operated vehicles (ROVs) and autonomous underwater vehicles (AUVs). ROVs and AUVs have been used to track anthropogenic effects on the ocean, with the potential to monitor changes in the ecosystem (Wynn *et al.*, 2014; Teoh *et al.*, 2018; Plum *et al.*, 2020; Sanchez *et al.*, 2020). These vehicles can commonly reach ranges of depths up to 6 km (Wynn *et al.*, 2014), although examples such as the *Nereus* have approached 11 km (WHOI, 2014). However, in many cases these technologies are still limited by their power consumption

and cannot be used in more environmentally sensitive areas of the ocean, where the vehicles could potentially produce or incur damage (Page *et al.*, 2017). Such areas include small crevices, or even open spaces where natural debris can cause vehicle damage (Teoh *et al.*, 2018; Plum *et al.*, 2020). As an alternative tool, biologically inspired AUVs offer advantages that address such limitations, including high power consumption and disruptive wake signatures (Fish, 2020). These bioinspired vehicles use animal body forms and principles, within the broader frame of biomimicry.

Bioinspired robotics study the biological systems that act as models from which machines are designed. Biological systems are adapted to selective pressure and environmental conditions (Darwin, 1859), and engineers can apply these natural designs to address similar engineering problems (Fish, 2020). Within bioinspired robotics, biohybrid approaches integrate both biological and robotic components (Yang *et al.*, 2018). These biological constructs have the capability both to improve robotics by taking advantage of existing tools in nature, and to use engineering tools to advance our knowledge of the natural world.

At present, there are two approaches to building biohybrid systems. The first is to incorporate live cells or tissues (Nawroth *et al.*, 2012; Morimoto *et al.*, 2018). Ricotti *et al.* (2017) describes this bottom-up approach for a comprehensive list of devices actuated by living cells, from bacteria and motile cells, cardiomyocytes, skeletal muscles, and insect self-contractile tissues. These approaches offer advantages, such as increased controllability and new potentials in environmental sensing, but require specific media for survival (Webster *et al.*, 2016a and 2016b; Morimoto *et al.*, 2018). Another approach is to integrate electronics into live insects (Sato and Maharbiz, 2010; Dirafzoon *et al.*, 2015; Latif *et al.*, 2016; Li and Sato, 2018; Saha *et al.*, 2020; Tadepalli *et al.*, 2020) and higher order animals (Valero-Sarmiento *et al.*, 2017). The external control of insect locomotion has incited a growing collection of "cyborg" cockroaches (Holzer and Shimoyama, 1997; Bozkurt *et al.,* 2016; Latif and Bozkurt, 2017), beetles (Sato *et al.*, 2009; Cao *et al.*, 2016; Li *et al.*, 2016; Vo Doan *et al.*, 2018; Li *et al.*, 2018; Cao and Sato, 2019), and moths (Bozkurt *et al.*, 2009; Tsang *et al.*, 2010).

The control of aquatic animals has additional potentials for robotics. First, as previously described, biohybrid swimming robots can expand ocean monitoring to areas which traditional AUVs and ROVs cannot reach because of size constraints, damage to the vehicle, or impact on the wildlife (Teoh *et al.*, 2018; Plum *et al.*, 2020). Second, using marine invertebrates offers insights into modes of locomotion that arose early in the evolutionary history of animals (Halanych, 2015).

Animal models for aquatic vehicles

The choice of model organism offers different advantages and disadvantages in design considerations for bioinspired aquatic vehicles. For example, although large fishes and manta rays can travel fast speeds over long distances (Fish, 2020), the integration of robotic control onto these organisms requires extensive training, personnel, and access to these animals, which introduce more ethical considerations. Although aquatic invertebrates may swim slower and be more affected by the weight and buoyancy of self-contained robotic devices, these invertebrates offer advantages in their simplicity. Jellyfish offer additional benefits because of their low cost of transport (COT), one metric of energy efficiency defined

as the mass-specific energy input per distance traveled (Gemmell *et al.*, 2013).

Jellyfish as a model organism

Cnidarian jellyfish fossils have revealed the conservation of the medusan body structure since the Middle Cambrian period, despite over 505 million years of evolutionary pressure (Cartwright *et al.,* 2007). Because the jellyfish bell structure and locomotion are linked to multiple behaviors, including feeding and escaping from predators (Arai, 1997), jellyfish swimming provides a unique model for evolutionary and ecological insights.

In addition to the energy efficiency exhibited by natural jellyfish, biohybrid robotic jellyfish offer new advantages to robotics because jellyfish are naturally found in a variety of environments, including thousands of meters below surface (the limit of current ocean exploration depths), which the animals can traverse without a swim bladder for pressure equilibration (NOAA, 2016). Although jellyfish are relatively slow swimmers with speeds on the order of cm/s, some species such as *Stomolopus meleagris* can exhibit directional swimming, migration, and maintain position against tidal currents, which are useful traits for an underwater vehicle (Shanks and Graham, 1987).

The microelectronic systems described in this protocol can increase swimming speeds up to threefold (Xu and Dabiri, 2020; Xu *et al.*, 2020a). Moreover, because AUVs and ROVs have demonstrated high speeds on field tests (traveling on the order of m/s), both traditional and new biohybrid tools can be used synergistically for future deployments, where AUVs and ROVs can tow biohybrid robotic jellyfish to certain environments before releasing the biohybrid robots into smaller spaces or areas in which the vehicles cannot reach. This can expand our current capabilities in ocean monitoring to provide new insights into the natural world and changing climate.

Furthermore, a major advantage of using jellyfish over animals such as manta rays and fish is their lower taxonomic order and relatively tractable nervous systems. Although further ethical considerations of invertebrate research are merited, jellyfish are invertebrates exempt from evaluation by an Institutional Animal Care and Use Committee. Even among jellyfish clades, scyphomedusae (true jellyfish) possess the most diffuse nervous system organization, comprising eight sensory structures and two nerve nets: the motor nerve net (MNN) and diffuse nerve net (DNN) (Arai, 1997; Satterlie, 2011; Katsuki and Greenspan, 2013). Thus, the moon jellyfish species *Aurelia aurita* offers advantages as simple model organisms that do not possess a centralized nervous system, brain, or pain receptors; and have potential capabilities that could benefit current underwater technologies.

Biology of Aurelia aurita (moon jellyfish)

Jellyfish are invertebrates with a simple body structure comprising a flexible bell and a muscle monolayer that lines the subumbrellar bell surface. Specifically, the moon jellyfish *Aurelia aurita* is a species of scyphozoa, the Cnidarian class of true jellyfish with medusae possessing radial symmetry about the oral-aboral body axis (Arai, 1997) and have the ability to exhibit directional travel, useful for underwater vehicles (Hamner *et al.*, 1994).

Jellyfish do not possess a centralized nervous system (CNS) or brain; rather, *A. aurita* have distributed,

non-polarized neuronal networks (Arai, 1997; Satterlie, 2011; Katsuki and Greenspan, 2013; Byrne, 2017). These nervous systems include eight rhopalia, a motor nerve net (MNN), and a diffuse nerve net (DNN). The rhopalia (also known as swim pacemakers or marginal sensory structures) are equally distributed in indentations along the bell margin and directly activate the MNN, which then activates bidirectional waves of muscle contractions. Stimulation of one rhopalium is sufficient to activate the entire MNN (Passano, 1965; Mackie and Meech, 1995).

To swim, jellyfish contract their ring-shaped musculature to decrease the volume of the subumbrellar cavity, thus expelling water and providing the motive force for acceleration (Satterlie, 2002), with additional suction-based propulsion from vortical structures (Gemmell *et al.*, 2015a). Oblate medusae such as *Aurelia* also rely heavily on the bell margin to create a paddling mode of locomotion (Colin and Costello, 2002; Costello *et al.*, 2020).

Jellyfish primarily move vertically using pulsed propulsion sufficient for survival, *i.e.*, passively catching prey, while their horizontal movement largely depends on ocean currents and waves (Satterlie, 2002). *A. aurita* also possess radial muscles that potentially contribute to non-symmetric thrust, thereby distorting individual vortex rings to cause turning maneuvers (Gemmell *et al.*, 2015b). Jellyfish are energetically efficient swimmers because of passive energy recapture, in which the animals still propel forward in a relaxed state without added energy input (Gemmell *et al.*, 2013; Gemmell *et al.*, 2018).

Robotic control of live jellyfish swimming

The following protocols describe the steps to build a biohybrid robotic jellyfish, comprising a microelectronic swim controller embedded in live *A. aurita* medusae, and subsequent laboratory and *in situ* experiments to calculate vertical swimming speeds. Design considerations include minimizing costs by using inexpensive off-the-shelf components, keeping the robotic system as compact and neutrally buoyant as possible, and using a two-electrode system and symmetric activation pattern to incite unidirectional swimming. See Figure 1 for representative images and schematics of the biohybrid robotic jellyfish and microelectronic system.

Using these methods, we have determined that the user control of jellyfish can increase their swimming speeds up to three times, both in the absence of flow (in the laboratory) and in coastal conditions (Xu and Dabiri, 2020; Xu *et al.*, 2020a). The existence of both faster and potentially more efficient swimming in jellyfish has implications for future studies in the ecology and evolution of basal organisms, beyond *A. aurita.* The results suggest that robotic systems can be used to uncover latent capabilities in organisms, and organisms can be used in biohybrid capabilities in ocean environments. Furthermore, biohybrid robotic jellyfish consume less external power per mass compared to other swimming robots in literature (Xu and Dabiri, 2020). This suggests that biohybrid designs can be used to improve the energy efficiency of robots to address extant challenges in robotics, which include power consumption and regeneration after damage (Yang *et al.*, 2018).

This work describes the entire process toward building and implementing a biohybrid robotic jellyfish, with a proof of concept that these constructs can be deployed in real ocean environments. This provides the basis for future practical applications in the ocean, with the ultimate goal to track markers of climate

www.bio-protocol.org/e3974

change. For comprehensive information on the usage and execution of these protocols, refer to Xu and Dabiri (2020) for the swim controller design and laboratory experiments, and Xu *et al.* (2020a) for field experiments.
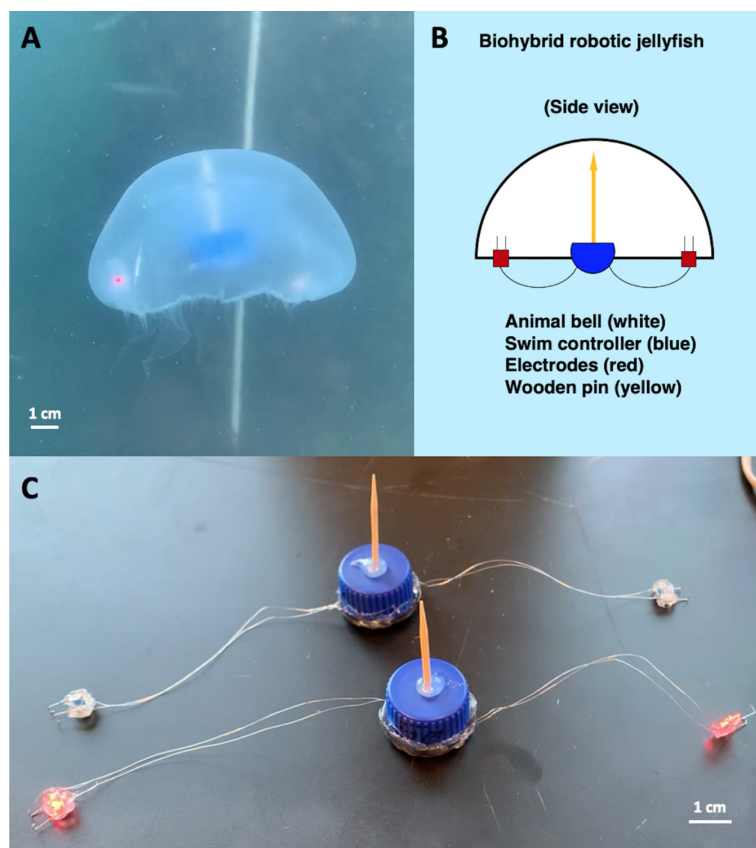

Figure 1. Biohybrid robotic jellyfish. A. Representative image of a biohybrid robotic jellyfish deployed in coastal conditions in the Atlantic Ocean. B. Schematic of the biohybrid robotic jellyfish to compare, with the animal bell labeled in white, swim controller housing in blue, two electrodes in red, and wooden pin in yellow. C. Two microelectronic swim controllers (front one is active, as shown by the red LEDs). Figures adapted from Xu *et al*. (2020a and 2020b).

Materials and Reagents

1. TinyLily mini processor (TinyCircuits, catalog number: ASM2101)
2. TinyLily light-emitting diodes (LED) 0402 (TinyCircuits, catalog number: ASL1001-LR)
3. 10-mAh ultra-light lithium polymer (LiPo) battery cell (PowerStream Technology, catalog number: PGEB201212)
4. Weights and buoyant materials (*e.g.*, stainless steel washers and cork)
5. Toothpicks (Good Old Values Bamboo Toothpicks, Pack of 1000)
6. Platinum rod, 254.0-μm diameter (A-M Systems, catalog number: 711000)
7. Polypropylene housing (*e.g.*, 2.11-cm diameter cap of a 15 ml Nunc™ conical centrifuge tube,

Thermo Scientific™, catalog number: 339650; and polypropylene plastic sheets cut to a corresponding circular shape)

8. Perfluoroalkoxy alkane (PFA)-coated silver wire, 76.2-μm diameter bare, 139.7-μm diameter coated (A-M Systems, catalog number: 785500)

9. Hot glue (*e.g.*, Gorilla hot glue sticks, Gorilla Glue)

10. Instant Ocean® Sea Salt (Instant Ocean, Spectrum Brands, catalog number: SS15-10, stored at room temperature)

Equipment

1. Soldering iron, solder, helping hands tool, and tweezers

2. Candle or open flame

3. Hot glue gun (*e.g.*, cordless hot glue gun, Neu Master, catalog number: FQ-009)

4. Parchment paper (*e.g.*, Quillon parchment paper, Uline, catalog number: S-19145)

5. Multimeter (*e.g.*, Fluke 115 Field Technicians Digital Multimeter)

6. Acrylic tank (Envision Acrylics, Inc., custom design with dimensions 1.8 m × 0.9 m × 0.9 m)

7. Refractometer (*e.g.*, Milwaukee MA871 Digital Brix Refractometer, catalog number: MW-MA871)

8. Ladder

9. Net (*e.g.*, a large fish net with a handle, or a custom-built fish net to match the dimensions of the bottom of the tank, with strings and handles to pull upward)

10. Plastic containers with lids (*e.g.*, 86 oz clear food storage container, Basix)

11. Insulated Styrofoam container (*e.g.*, Thermo Chill insulated carton with foam shipper, medium, 12" × 10" × 7", Polar Tech Industries, catalog number: 227C)

12. Cyber-shot DSC-RX100 (Sony, catalog number: DSCRX100/B)

13. Sony AX100 camera (Sony, catalog number: FDR-AX100)

14. Gates AX100 Underwater Housing (Gates Underwater Products, catalog number: AX100)

15. Background boards (*e.g.*, black foam board, 36 × 48", Uline, catalog number: S-19381 and white foam board 20 × 30 × 3/16" or 5 mm, Navy Penguin)

16. Rope tied to a dive weight

17. Zip ties (*e.g.*, red and yellow nylon zip ties)

18. SCUBA diving equipment (*e.g.*, mask, snorkel, fins, wetsuit, regulator, compressed air tanks, dive computer)

Software

1. Arduino (Arduino, https://www.arduino.cc/)

2. MATLAB (MathWorks, https://www.mathworks.com/)

3. ImageJ (National Institutes of Health, https://imagej.nih.gov/ij/)

Procedure

6

A. Building microelectronic swim controllers

1. Program the TinyLily microcontroller to the desired signal frequency, according to the manufacturer's instructions for uploading the code to the board using Arduino. Figure 2A shows the square pulse wave signal, with an amplitude of 3.7 V, pulse width of 10 ms, and adjustable frequency (f) and period (T).

   Note: Figure 2B shows an example of the Arduino code for a square pulse wave, with pulse width of 10 ms. Replace 'TIME' (highlighted in orange) with the desired period (T) in ms, i.e., for a frequency (f) of 0.50 Hz, T = 2,000 ms. For a two-electrode system, choose two stimulation pins, such as pins 2 and 3 shown in the example code in Figure 2B.
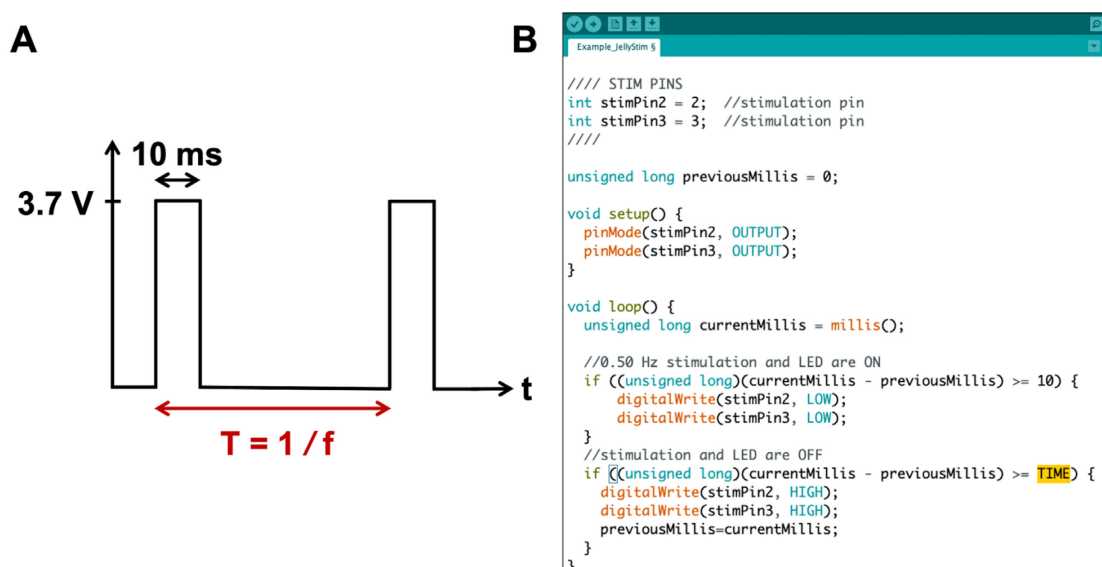

Figure 2. Electrical stimulation of jellyfish. A. A schematic of a square pulse wave to incite muscle contractions in *Aurelia aurita* moon jellyfish. The signal amplitude is 3.7 V and pulse width is 10 ms. The signal frequency (f) and period (T) can be adjusted, as desired. B. An example code that executes the signal in (A) using two stimulation pins, stimPins 2 and 3, which correspond to the yellow pins in Figure 3B. To adjust the signal frequency, replace 'TIME' (highlighted in orange) with the period in ms.

2. To build one electrode:

   a. Cut two pieces of PFA-coated silver wires to 10 cm in length, or at least half of the diameter of the jellyfish.

      Note: The animals used in prior experiments ranged from 9.8 to 19.0 cm in diameter.

   b. Flame both ends of the silver wires over an open flame to strip the PFA coating and expose the silver tip.

   c. Cut two pieces of platinum rod to 1 cm in length.

   d. Use a soldering iron, helping hand tools, and tweezers to maneuver the platinum rods, silver wires, and one LED into place (see Figure 3A for reference).

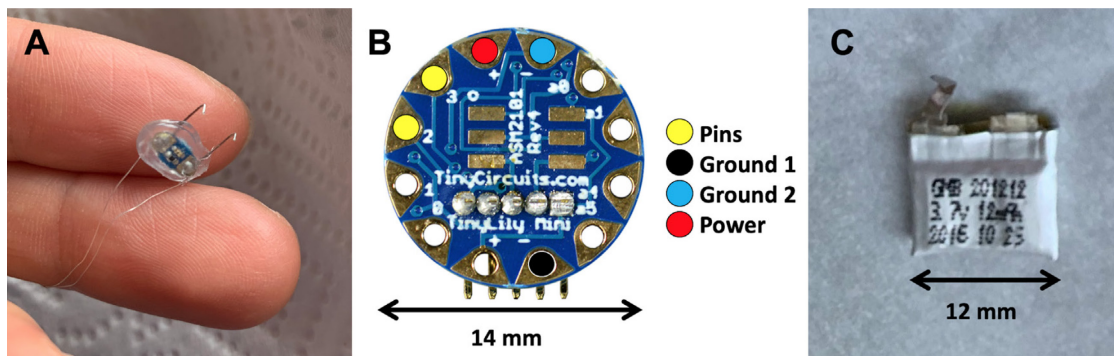*Note: Use higher temperatures, such as 450 °C or above, to improve the soldering process.*

Figure 3. Microelectronic components of the jellyfish swim controller. A. An electrode, comprising the following components: a red TinyLily LED, soldered platinum wire tips bent into a fishhook-like shape, soldered PFA-coated silver wires (connected to the microcontroller via yellow and black pins, as illustrated in B), and hot melt adhesive coating to waterproof. B. TinyLily microcontroller, with two stimulation pins labeled in yellow (pins 2 and 3), two ground pins labeled in black and cyan, and a power pin labeled in red. Photo credit to Tiny Circuits. C. Lithium polymer battery cell (Powerstream), active when connected to the red and blue pins in B.

e. Solder one end of each platinum rod to the positive and negative terminals of the LED.

f. Solder one exposed end of each silver wire to the LED terminals.

g. Use hot melt adhesive to coat the LED to seal the solder connections.

  i. Squeeze a thin strip of hot melt adhesive directly onto the parchment paper and place the LED onto the glue. The parchment paper will not stick to the adhesive.

  ii. Press the electrode gently into the adhesive to ensure the surface is covered.

  iii. Wait for the adhesive to dry (approximately 1 min), and use the tweezers to pick up the electrode, which is now coated on one side.

  iv. Squeeze another thin strip of hot melt adhesive onto the parchment paper.

  v. Press the other side of the electrode into the adhesive to ensure the surface is covered.

  vi. Wait for the adhesive to dry, and trim excess glue as needed.

  vii. Ensure that no solder is exposed to the air.

  Note: Exposed solder will increase hydrogen bubble production during electrolysis, which can cause tissue damage to the jellyfish mesoglea over prolonged periods.

h. Use the tweezers to bend the platinum rods into a fishhook-like shape, as shown in Figure 3A.

3. Repeat Step A2 to build multiple electrodes.

4. Trim a toothpick, removing at least 1/3 of the total length and keeping the remainder. The length of this remaining piece can be adjusted as desired, according to the depth of tissue in the jellyfish manubrium.

5. Use hot melt adhesive to attach the blunt end of the toothpick to the cylindrical plastic housing, as shown in Figure 1C for reference.

6. Solder the exposed silver wire connected to the negative terminal of the electrode onto the TinyLily ground pin (labeled in black in Figure 3B). Multiple wires can be soldered to this ground pin.

7. Solder the exposed silver wire connected to the positive terminal of the electrode onto the TinyLily stimulation pin (for the two-electrode example, solder one wire onto pin 2 and the other onto pin 3, shown in yellow in Figure 3B).
    Note: Use a multimeter to test the connections.

8. Solder the positive and negative terminals of the LiPo battery (Figure 3C) onto the corresponding terminals on the Tiny Lily (labeled in red and blue in Figure 3B).
    The LEDs will flash while the signal is on, as a visual confirmation that the swim controller is active. Figure 1C shows an example of an active swim controller with red LED electrodes.
    Note: Take care not to short the battery when soldering. One technique is to apply shrink wrap or other nonconductive materials to the battery leads. Avoid using the same ground terminal as used in Step A6.

9. Optional: Wrap tape around the microcontroller and battery to secure all the connections in place before attaching to the plastic housing.

10. Use hot melt adhesive to secure the central electronics (soldered microcontroller and battery unit) into the cylindrical plastic housing (centrifuge cap). Ensure that the electrodes and electrode wires are outside of the housing.

11. Use hot melt adhesive to secure the flat circular plastic piece onto the cylindrical piece, as shown in Figure 4.
    Note: Ensure that the electrode wires are oriented evenly outward from the central housing before attaching the flat piece. Once the housing is secured with adhesive, removing the electronics will damage the silver wires and potentially break the connection to the electrodes.
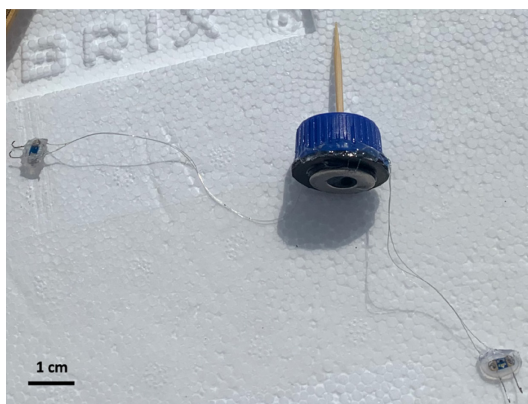

Figure 4. Side view of a two-electrode swim controller to show the flat polypropylene piece (black), with a silver washer to ballast the system. Scale bar, 1 cm.

12. Offset the weight of the microelectronics accordingly by using washers and/or cork until the entire microelectronic system is neutrally buoyant in the desired saltwater, as shown in Figure 4.

Note: It is helpful to determine the buoyancy on an inactive swim controller before assembling these devices. Nevertheless, because A. aurita are sensitive to changes in buoyancy, fully assembled devices should be retested in the appropriate water conditions, i.e., salt concentration and temperature of the water to maintain neutral buoyancy. In addition, changing the ballast of the swim controller can determine the orientation for improved unidirectional swimming stability, i.e., the swim controller was designed to be top heavy for swimming downward to the bottom of the tank (Xu and Dabiri, 2020), and bottom heavy for swimming upward to the ocean surface (Xu et al., 2020a).

B. Inserting the swim controller into the jellyfish
   1. Place a jellyfish subumbrellar surface upward in a container filled with saltwater.
   2. Insert the toothpick through the manubrium so that the plastic housing is placed directly on the stomachs and oral arms. Ensure that the entire wooden pin is embedded securely in the jellyfish.
   3. Use one hand to hold the jellyfish bell securely. Use the other hand to embed one electrode into the jellyfish, and a curved hand motion to secure the fishhook-shaped platinum rod tips into the tissue.
      a. Embedding the electrode should be conducted as swiftly as possible to avoid excessive motion from the animal, which can cause the electrodes to pull on the tissue.
      b. The optimal location to embed is toward the margin, from the underside of the animal. Because the marginal tissue is thin, embedding the electrode at a radial distance between the margin (radius R) and halfway inward (radius R/2) is sufficient.
      c. Proper technique ensures a tight hold in the jellyfish tissue and requires additional effort to remove the device from the animal. If the electrode is not embedded well into the tissue, or if the electrode falls out of the animal, repeat the process again until there is a secure hold. Avoid embedding directly into the same location, which can cause excessive tissue damage that can preclude proper electrode insertion.
   4. Repeat Step B3 for multiple electrodes. Ensure that the electrodes are spaced evenly, *i.e.*, for a two-electrode system, the electrodes should be embedded symmetrically in the animal (see Figure 1A).

C. Conducting straight free-swimming experiments in the laboratory
   1. Fill the tank with DI water.
   2. Add Instant Ocean salt mix to the desired salinity (35 ppt).
      a. To begin adding the salt, first estimate the amount of salt mix needed, assuming no impurities as a conservative estimate (Arain, 2020).
      Note: Add the salt mix into DI water. Adding DI water into the salt mix can form calcium

precipitates, which can result in cloudy water.

   b. Measure the salinity using a refractometer, and add more salt mix accordingly.

   c. Mix the water well, ideally using an automatic pump to recirculate the water.

   d. Let equilibrate for at least a few hours, ideally overnight.

   e. Measure the salinity using a refractometer, and adjust the salt or water content accordingly.

   f. Use towels or other cleaning tools to remove air bubbles from the sides of the tank.

3. Acclimate the jellyfish (without embedded swim controllers) to the water for at least 4 h, up to overnight. This will ensure that the tissue density is approximately neutral with the surrounding water.

4. Optional: Place a net on the bottom of the 1.8-m length tank to collect the jellyfish post-experiments.

   Note: Because the animals will be initiated from the top of the tank and swim downward, these experiments are most easily conducted using batches of multiple animals. For successive runs, biohybrid robotic jellyfish from previous trials remain at the bottom of the tank until all animals are tested. Use the net to bring all animals to the top of the tank to remove, then wait at least 30 min for the water to return to static conditions, as described in Steps C10 to C12.

5. Set up a camera, *e.g.*, 1,920 × 1,080 resolution at 60 fps on the Cyber-shot DSC-RX100, as shown in Figure 5 to record videos of the animals swimming.
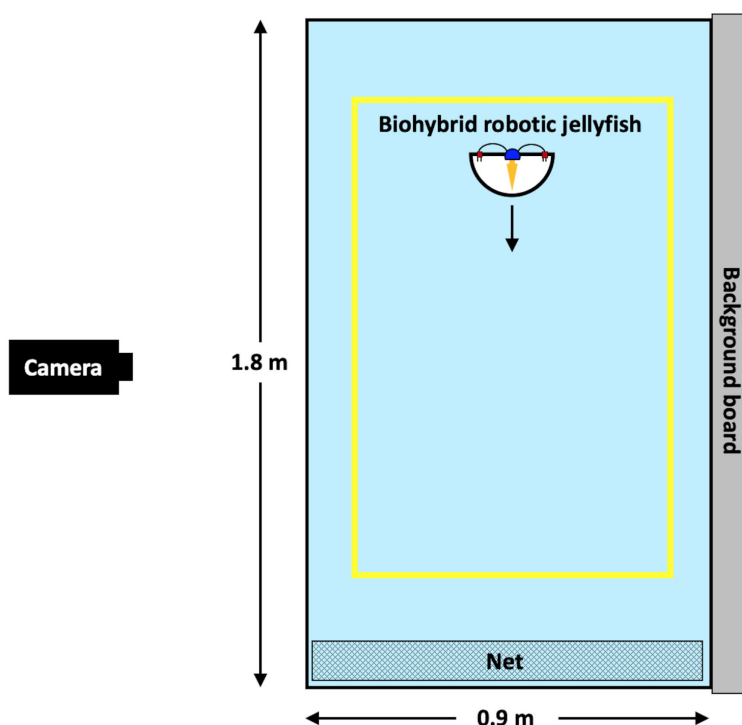

Figure 5. Laboratory setup for vertical swimming experiments. The setup for laboratory experiments to calculate the vertical swimming speed of biohybrid robotic jellyfish includes the following components: a 1.8-m tall acrylic tank filled with saltwater (35 ppt), background board (black or white) attached to the back panel of the tank, biohybrid robotic jellyfish (swimming

downward, initiated from the top of the tank), optional net at the bottom of the tank to facilitate removing the jellyfish from the tank post-experiments, and camera to record videos. The yellow box highlights the area of the tank in which the animal is away from the sides, top, and bottom of the tank, which can minimize disturbances from wall effects.

6. Tape the background boards to the outside of the tank's back panel, as shown in Figure 5. This will ensure that the background is a uniform color and simplify the data analysis.
   Note: To track the swim controller, use a white board so that the swim controller housing is maximally visible through semi-transparent animal (Figure 8A). To track the whole animal, use a black board with adequate lighting on the animal tissue, which will appear to be an opaque white (Figure 8B). Tracking the entire animal can allow for additional analysis of the geometric parameters, such as the time-dependent diameter of the animal throughout the swimming cycle or time periods of contraction and relaxation.

7. Use a ladder to access the top of the tank. Insert an active microelectronic swim controller into the jellyfish, as described in Procedure B, while the animal is at the top of the tank.

8. Hold the animal with both hands at the top of the tank, and wait for the water to become relatively quiescent, approximately 2 min.

9. Slowly release the animal, taking care to minimally disturb the water. Allow the animal to swim downward to the bottom of the tank.

10. Wait at least 5 to 15 min between successive trials to allow the water to return to quiescent conditions, depending on the amount of disturbance generated by the biohybrid robotic jellyfish.

11. Repeat Steps C7 to C10 for additional animals.

12. Once all animals are at the bottom of the tank, use the net to capture all biohybrid robotic jellyfish to the surface, and remove from the tank.

13. For additional trials, wait at least 30 min to allow the water to return to quiescent conditions, depending on the amount of disturbance generated by the biohybrid robotic jellyfish and net.

14. Repeat Steps C7 to C13 until all experimental parameters are tested (*e.g.*, frequencies ranging from 0.25 to 1.00 Hz and control cases with inactive swim controllers at 0 Hz), as described in Xu and Dabiri (2020). After all trials are completed, proceed to Procedure E for post-experimental steps.

D. Conducting straight free-swimming experiments *in situ* (coastal conditions)
   1. Prepare for field experiments.
      a. Attach colored zip ties onto the dive rope with alternating colors (red and yellow) spaced 30.5 cm. Trim the excess zip tie material. The remainder attached to the rope serves as background markers for data analysis.
      b. Tie a dive weight (*e.g.*, 2.5 kg) to one end of the rope.
      c. Insert an active microelectronic swim controller into the jellyfish, as described in Procedure B, with each animal in an individual plastic container filled with saltwater that matches the

field conditions (see Figure 6C).

d. Cover the plastic container with its corresponding lid.

Note: Ensure that the plastic containers are overfilled with saltwater to minimize the presence of air bubbles that could negatively impact the jellyfish.

e. Place the plastic containers in an insulated box to carry into the field (Figure 6B). Ensure that the containers are secured and do not shift within the box; if the containers move freely, include padding or other filler materials.

Note: Bring extra swim controllers (embedded in foam for protection), animals, battery-powered soldering irons, scissors, and other useful tools into the field.

f. Place the camera in the waterproof plastic casing, *e.g.*, Sony AX100 camera in the Gates AX100 Underwater Housing.

2. Allow two SCUBA divers to prepare their gear and enter the water (labeled 'Divers 1 and 2'), as shown in Figure 6A.

3. Allow one person to stay on shore or a dock, with the biohybrid robotic jellyfish and other experimental materials and equipment (labeled 'Person on shore'), as shown in Figure 6A.

Figure 6. Field experiments conducted in coastal conditions in Woods Hole, MA. A. Swimming experiments in the coastal waters of MA required two SCUBA divers and one person on shore. The person on shore can tie the rope to the dock post and maneuver the biohybrid robotic jellyfish to one diver (illustrated in D), who can release the jellyfish at the bottom of the ocean near the rope as a background feature. The second diver can record videos of the

biohybrid robotic jellyfish. B. Biohybrid robotic jellyfish were transported in plastic containers, stored in an insulated Styrofoam box, with extra swim controllers embedded in foam. C. An image of one biohybrid robotic jellyfish in the plastic container. D. A diver holding a container with a biohybrid robotic jellyfish in preparation for vertical swimming experiments. Note that the rope with red and yellow markers is visible, secured to the wooden dock post.

4. Diver 1: Place the weighted end of the rope on the ocean floor for coastal experiments, as shown in Figure 7.
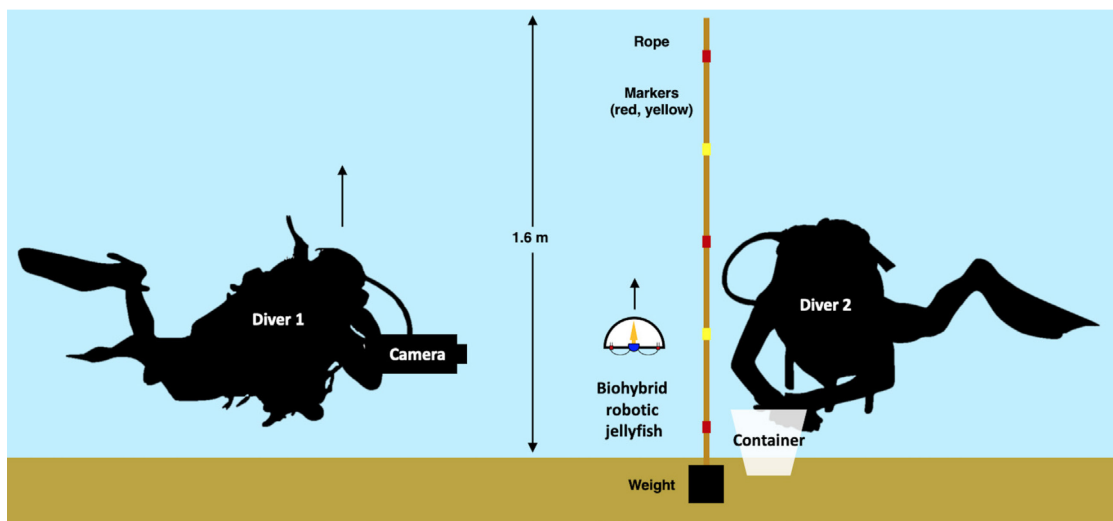

Figure 7. Field setup for vertical swimming experiments. The setup for *in situ* experiments in coastal conditions to calculate the vertical swimming speed of biohybrid robotic jellyfish includes the following components: a rope with alternating red and yellow markers, weighted to the bottom of the ocean and securely fashioned to the surface; one diver with an underwater camera setup to record videos of the trials; a second diver to maneuver the animal into its initial position at the ocean bottom using a container; and the biohybrid robotic jellyfish, swimming upward.

5. Person on shore: Tie the other end of the rope to the dock or other surface structure, ensuring that the rope is taut to minimize rope motion. The rope should be visible in the background of recorded videos for data analysis (1,920 × 1,080 resolution at 30 fps).

6. Person on shore: Remove the lid and hand a plastic container with one of the biohybrid robotic jellyfish to Diver 2, as shown in Figure 6D.

7. Diver 2: Gently submerge the plastic container into the water, taking care to ensure that the microelectronic system is still fully embedded in the jellyfish. Move the container to the bottom of the ocean, near the background rope. Gently release the biohybrid robotic jellyfish and ensure that the animal is oriented properly for forward swimming.

8. Diver 1: Record a video of the biohybrid robotic jellyfish, taking care to minimize diver and camera motion and keep the rope markers visible in the background. Track the jellyfish from the

ocean floor to surface (1.6 m) if possible, with minimal motion in the depth axis of the camera (in and out of the image plane).

9. Diver 2: Once the animal reaches the ocean surface, capture the biohybrid robotic jellyfish in the plastic container and hand the container back to the person on shore.

10. Person on shore: To obtain control cases, cut the electrode wires, taking care to ensure that all microelectronics are still strongly embedded into the animal. Hand the biohybrid robotic jellyfish in the plastic container back to Diver 2.

    a. Control cases are defined as trials in which the swim controller is embedded but inactive (0 Hz) to determine each animal's baseline swimming frequency and speed.

11. Divers 1 and 2: Repeat Steps D7 to D9.

12. Repeat Steps D6 to D11 for additional animals. After all trials are completed, proceed to Procedure E for post-experimental steps.

E. Conducting post-experimental procedures

1. Remove the electrodes from the animals by gently following the curvature of the fishhook-like platinum rods to minimize tissue damage.

2. Remove the plastic housing by gently pulling the wooden pin from the manubrium.

3. Return the animals to their housing conditions.

4. Feed the animals (such as with *Artemia* nauplii) to encourage recovery.

Data analysis

A. Calculate the unidirectional swimming speed and enhancement factor of biohybrid robotic jellyfish using MATLAB

1. Convert videos to images.

2. Use ImageJ to obtain the diameter of the animal, swim controller housing, and other relevant geometric parameters (if desired) in pixels. (The diameters of the animal and housing are known quantities in centimeters.)

3. Find the (x, y) centroids of the jellyfish swim controller (Figure 8A) for all frames, time t, in pixels ($cap_{x,t}$, $cap_{y,t}$).

Note: If using color images, split the image into its red, green, and blue components and filter for the appropriate size and color of the swim controller housing, i.e., blue in Figure 8A. If using a dark background in laboratory experiments, find the (x, y) centroids of the jellyfish, filtering for bright pixels to obtain the opaque white tissue (Figure 8B).
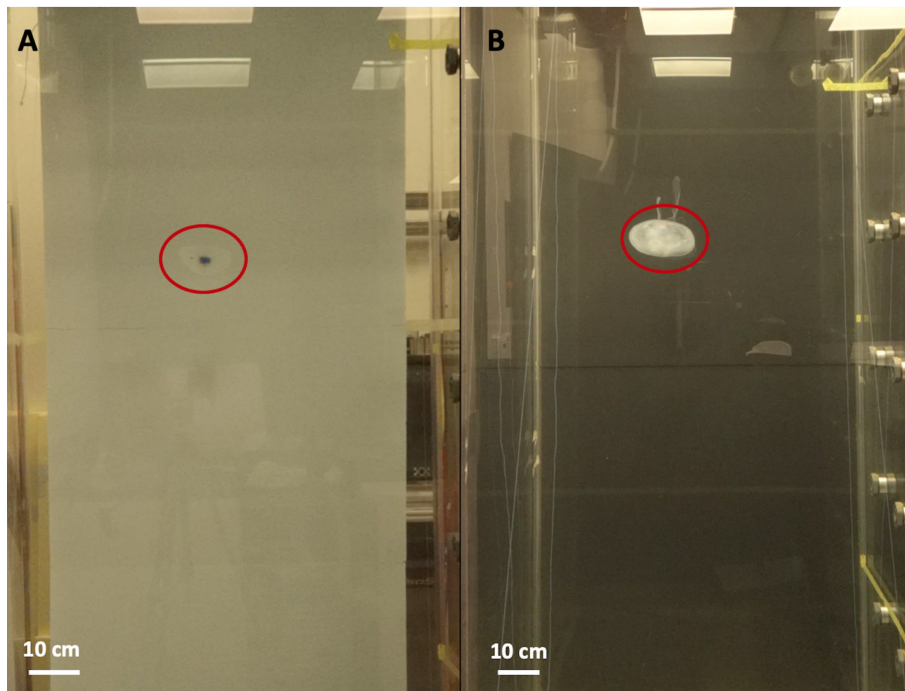
Figure 8. Representative images of laboratory conditions. A. A biohybrid robotic jellyfish (circled in red) swimming downward in the tank. Note that the semi-transparent jellyfish tissue blends in with the white background, allowing the swim controller to be visible for tracking. B. A biohybrid robotic jellyfish (circled in red) swimming downward in the tank. Note that the jellyfish tissue is white against the black background, which allows for the animal bell and morphological parameters to be tracked. For clarity, reflections and other aspects of the tank are also visible, including side ports (far right). Scale bars, 10 cm.

4. Calculate the vertical displacements for laboratory experiments, in which the camera is stationary:
   a. Calculate the vertical displacement (distance between the centroid and the initial starting centroid) for each frame: $d_t = \mathrm{cap}_{y,t} - \mathrm{cap}_{y,0}$
   b. Convert the displacements from pixels to centimeters by using a known scale in the image, such as the diameter of the swim controller housing (2.11 cm), or other methods of camera calibration.

   Note: Select video segments in which the animal is in center of the tank, and track vertical displacements only for the middle half of the tank (see yellow box in Figure 5). This will minimize wall effects from the animal swimming too close to the sides or bottom of the tank, and from water disturbances at the top and bottom of the tank from initializing the experiment or other animals pulsing at the bottom of the tank from previous trials.

5. Calculate the vertical displacements for *in situ* experiments, in which camera motion is nonzero:
   a. Find the (x, y) centroids of the rope markers in the background, in pixels ($\mathrm{marker}_{x,t}$, $\mathrm{marker}_{y,t}$).
      Note: Use the same technique above, filtering for the appropriate sizes and colors of the

rope markers, i.e., red and yellow in Figure 9.

Figure 9. Representative image from *in situ* experiments. A biohybrid robotic jellyfish in field conditions, with the background markers (red and yellow) on the rope visible.

b. Determine the (x, y) centroids of the jellyfish relative to the background rope markers ($norm\_cap_{x,t}$, $norm\_cap_{y,t}$).

   Note: Because MATLAB's image origin is defined as the top left corner, the equation should be $norm\_cap_{x,t} = cap_{x,t} - marker_{x,t}$ for the x-components and $norm\_cap_{y,t} = marker_{y,t} - cap_{y,t}$ for the y components.

c. Calculate the vertical displacement (distance between the centroid and the initial starting centroid) for each frame: $d_t = norm\_cap_{y,t} - norm\_cap_{y,0}$.

d. Convert the displacements from pixels to centimeters by using a known scale in the image, such as the distance between subsequent rope markers (30.5 cm), or other methods of camera calibration.

   i. Calculate the distance in pixels between subsequent rope markers, if multiple rope markers are visible. If multiple rope markers are not visible, mark the distance as not a number (NaN).

   ii. Interpolate between the distances to fill in NaN values.

Note: Select video segments in which the animal is toward the middle of the ocean depth, avoiding the ocean bottom and surface (see note in the above step 4).

6. Calculate the differential swimming speeds, using the distance between each subsequent pair of time steps ($d_{t+1} - d_t$) and multiplying by the camera framerate, *e.g.*, 60 fps in the laboratory experiments and 30 fps in the field experiments.

7. Calculate the mean swimming speed (*v*).

8. Optional: Calculate the normalized swimming speed, or proficiency, by dividing the absolute swimming speed by the diameter of the animal (*D*): $v_{norm} = v/D$.

9. Calculate the enhancement factor by dividing the mean swimming speed (absolute or

normalized, as previously described) by the baseline swimming speed (the swimming speed of the control case, in which the animal is initiated with an inactive swim controller, 0 Hz).

Note: Additional information is described for laboratory experiments in Xu and Dabiri (2020) and for field experiments in Xu et al. (2020a).

Acknowledgments

Competing interests

The authors declare no competing interests.

Ethics

A. aurita are invertebrates that do not possess a brain, central nervous system, pain receptors, or nociceptors, and therefore do not require protocol review or approval from the Institutional Animal Care and Use Committee (IACUC). However, we took great care to ensure the welfare interests of these animals, in accordance to the precautionary and minimization principles to reduce the number of animals used and refine procedures to minimize potential distress. We also monitored the jellyfish and microelectronic systems to ensure that we introduced no additional electronic waste or other material into the ocean. Further information about our ethical views can be found in Xu *et al.* (2020b).

References

1. Arai, M. N. (1997). A functional biology of scyphozoa. London: Chapman & Hall.
2. Arain, H. M. (2020). Direct salt addition calculator. Hamza's Reef.
3. Bozkurt, A., Lal, A. and Gilmour, R. (2009). Aerial and terrestrial locomotion control of lift assisted insect biobots. *Annu Int Conf IEEE Eng Med Biol Soc* 2009: 2058-2061.
4. Bozkurt, A., Lobaton, E. and Sichitiu, M. (2016). A biobotic distributed sensor network for under rubble search and rescue. *IEEE Computer, Special Issue Emergency Response* 49(5): 38-46.
5. Byrne, J. H., editor. (2017). The Oxford Handbook of Invertebrate Neurobiology. Oxford University Press.
6. Cao, F., Zhang, C., Choo, H. Y. and Sato, H. (2016). Insect–computer hybrid legged robot with

user- adjustable speed, step length and walking gait. *J R Soc Interface* 13(116): 20160060.

7. Cao, F. and Sato, H. (2019). Insect–computer hybrid robot achieves a walking gait rarely seen in nature by replacing the anisotropic natural leg spines with isotropic artificial leg spines. *IEEE Trans Robot* 35(4): 1034-1038.

8. Cartwright, P., Halgedahl, S. L., Hendricks, J. R., Jarrard, R. D., Marques, A. C., Collins, A. G. and Lieberman, B. S. (2007). Exceptionally preserved jellyfishes from the Middle Cambrian. *PLoS ONE* 2(10): e1121.

9. Darwin, C. (1859). On the origin of species by means of natural selection, or preservation of favoured races in the struggle for life. London: John Murray.

10. Colin, S. P. and Costello, J. H. (2002). Morphology, swimming performance and propulsive mode of six co-occurring hydromedusae. *J Exp Biol* 205(Pt 3): 427-437.

11. Costello, J. H., Colin, S. P., Dabiri, J. O., Gemmell, B. J., Lucas, K. N. and Sutherland, K. R. (2020). The Hydrodynamics of Jellyfish Swimming. *Ann Rev Mar Sci*.

12. Dirafzoon, A., Bozkurt, A. and Lobaton, E. (2015). Dynamic topological mapping with biobotic swarms. arXiv. 1507.03206v2. https://arxiv.org/abs/1507.03206.

13. Fish, F. E. (2020). Advantages of aquatic animals as models for bio-inspired drones over present AUV technology. *Bioinspir Biomim* 15(2): 025001.

14. Gemmell, B. J., Costello, J. H., Colin, S. P., Stewart, C. J., Dabiri, J. O., Tafti, D. and Priya, S. (2013). Passive energy recapture in jellyfish contributes to propulsive advantage over other metazoans. *Proc Natl Acad Sci U S A* 110(44): 17904-17909.

15. Gemmell, B. J., Colin, S. P., Costello, J. H. and Dabiri, J. O. (2015a). Suction-based propulsion as a basis for efficient animal swimming. *Nat Commun* 6: 8790.

16. Gemmell, B. J., Troolin, D. R., Costello, J. H., Colin, S. P. and Satterlie, R. A. (2015b). Control of vortex rings for manoeuvrability. *J R Soc Interface* 12(108): 20150389.

17. Gemmell, B. J., Colin, S. P. and Costello, J. H. (2018). Widespread utilization of passive energy recapture in swimming medusae. *J Exp Biol* 221(Pt 1).

18. Halanych, K. M. (2015). The ctenophore lineage is older than sponges? That cannot be right! Or can it? *J Exp Biol* 218(4): 592-597.

19. Hamner, W. M., Hamner, P. P. and Strand, S. W. (1994). Sun-compass migration by *Aurelia aurita* (Scyphozoa): population retention and reproduction in Saanich Inlet, British Columbia. *Mar Biol* 119(3): 347-356.

20. Holzer, R. and Shimoyama, I. (1997). Locomotion control of a bio-robotic system via electric stimulation. In: *Proceedings of the 1997 IEEE/RSJ International Conference on Intelligent Robot and Systems. Innovative Robotics for Real-World Applications*. IROS '97.

21. Katsuki, T. and Greenspan, R. J. (2013). Jellyfish nervous systems. *Curr Biol* 23(14): R592-594.

22. Kim, S. K. and Pallela, R. (2012). Medicinal foods from marine animals. In: *Marine Medicinal Foods - Impli- cations and Applications - Animals and Microbes*, pages 1-9. Elsevier.

23. Latif, T. and Bozkurt, A. (2017). Roach biobots: toward reliability and optimization of control. *IEEE Pulse* 8(5): 27-30.

24. Latif, T., Whitmire, E., Novak, T. and Bozkurt, A. (2016). Sound localization sensors for search and rescue biobots. *IEEE Sens J* 16(10): 3444-3453.

25. Li, Y. and Sato, H. (2018). Insect-computer hybrid robot. *Mol Front J* 02(01): 30-42.

26. Li, Y., Wu, J. and Sato, H. (2018). Feedback control-based navigation of a flying insect-machine hybrid robot. *Soft Robotics* 5(4): 365-374.

27. Li, Y., Cao, F., Thang Vo Doan, T., and Sato, H. (2016). Controlled banked turns in coleopteran flight measured by a miniature wireless inertial measurement unit. *Bioinspir Biomim* 11(5): 056018.

28. Mackie, G. and Meech, R. (1995). Central circuitry in the jellyfish *Aglantha*. II: The ring giant and carrier systems. *J Exp Biol* 198(11): 2271-2278.

29. Malve, H. (2016). Exploring the ocean for new drug developments: Marine pharmacology. *J Pharm Bioallied Sci* 8(2): 83-91.

30. Morimoto, Y., Onoe, H., and Takeuchi, S. (2018). Biohybrid robot powered by an antagonistic pair of skeletal muscle tissues. *Sci Robot* 3(18): eaat4440.

31. Nawroth, J. C., Lee, H., Feinberg, A. W., Ripplinger, C. M., McCain, M. L., Grosberg, A., Dabiri, J. O. and Parker, K. K. (2012). A tissue-engineered jellyfish with biomimetic propulsion. *Nat Biotechnol* 30(8): 792-797.

32. NOAA. (2016). NOAA Ship Okeanos Explorer: 2016 Overview: NOAA Office of Ocean Exploration and Research. National Oceanic, and Atmospheric Administration. US Department of Commerce.

33. NOAA. (2020a). What is ocean exploration and why is it important? National Oceanic, and Atmospheric Administration.

34. NOAA. (2020b). Why should we care about the ocean? National Oceanic, and Atmospheric Administration.

35. Page, B. R., Ziaeefard, S., Pinar, A. J. and Mahmoudian, N. (2017). Highly maneuverable low-cost underwater glider: Design and development. *IEEE Robot Auto Let* 2(1): 344-349.

36. Passano, L. M. (1965). Pacemakers And Activity Patterns In Medusae: Homage To Romanes. *Am Zool* 5: 465-481.

37. Plum, F., Labisch, S. and Dirks, J. H. (2020). SAUV-A Bio-Inspired Soft-Robotic Autonomous Underwater Vehicle. *Front Neurorobot* 14: 8.

38. Ricotti, L., Trimmer, B., Feinberg, A. W., Raman, R., Parker, K. K., Bashir, R., Sitti, M., Martel, S., Dario, P. and Menciassi, A. (2017). Biohybrid actuators for robotics: A review of devices actuated by living cells. *Sci Robot* 2(12).

39. Roboroach, The RoboRoach Bundle. https://backyardbrains.com/products/roboroach.

40. Saha, D., Mehta, D., Atlan, E., Chandak, R., Traner, M., Lo, R., Gupta, P., Singamaneni, S., Chakrabartty, S., and Raman, B. (2020). Explosive sensing with insect-based biorobots. *bioRxiv.* https://doi.org/10.1101/2020.02.10.940866.

41. Sanchez, P. J. B., Papaelias, M. and Marquez, F. P. G. (2020). Autonomous underwater vehicles: Instrumentation and measurements. *IEEE Instru Meas Mag* 23(2): 105-114.

www.bio-protocol.org/e3974

42. Sato, H., Peeri, Y., Baghoomian, E., Berry, C. W. and Maharbiz, M. M. (2009). Radio-controlled cyborg beetles: A radio- frequency system for insect neural flight control. In: *2009 IEEE 22nd International Conference on Micro Electro Mechanical Systems*.

43. Sato, H. and Maharbiz, M. M. (2010). Recent developments in the remote radio control of insect flight. *Front Neurosci* 4: 199.

44. Satterlie, R. A. (2002). Neuronal control of swimming in jellyfish: a comparative story. *Can J Zool* 80(10): 1654-1669.

45. Satterlie, R. A. (2011). Do jellyfish have central nervous systems? *J Exp Biol* 214(Pt8): 1215-1223.

46. Shanks, A. L. and Graham, W. M. (1987). Orientated swimming in the jellyfish *Stomolopus meleagris* L. Agassiz (Scyphozoan: Rhizostomida). *J Exp Mar Biol Ecol* 108(2): 159-169.

47. Tadepalli, S., Cao, S., Saha, D., Liu, K.-K., Chen, A., Bae, S. hyun, Raman, B., and Singamaneni, S. (2020). Remote-controlled insect navigation using plasmonic nanotattoos. *bioRxiv*. https://doi.org/10.1101/2020.02.10.942540.

48. Teoh, Z. E., Phillips, B. T., Becker, K. P., Whittredge, G., Weaver, J. C., Hoberman, C., Gruber, D. F. and Wood, R. J. (2018). Rotary-actuated folding polyhedrons for midwater investigation of delicate marine organisms. *Sci Rob* 3(20): eaat5276.

49. Tsang, W. M., Stone, A., Aldworth, Z., Otten, D., Akinwande, A. I., Daniel, T., Hildebrand, J. G., Levine, R. B., and Voldman, J. (2010). Remote control of a cyborg moth using carbon nanotube-enhanced flexible neuroprosthetic probe. In: *2010 IEEE 23rd International Conference on Micro Electro Mechanical Systems*.

50. Valero-Sarmiento, J. M., Reynolds, J., Krystal, A. and Bozkurt, A. (2017). *In Vitro* Evaluation of an Injectable EEG/ECG Sensor for Wireless Monitoring of Hibernation in Endangered Animal Species. *IEEE Sensors J* 18(2) 798-808. doi: 10.1109/JSEN.2017.2772844.

51. Vo Doan, T. T., Tan, M. Y. W., Bui, X. H. and Sato, H. (2018). An ultralightweight and living legged robot. *Soft Robotics* 5(1): 17-23.

52. Webster, V. A., Hawley, E. L., Akkus, O., Chiel, H. J. and Quinn, R. D. (2016a). Effect of actuating cell source on locomotion of organic living machines with electrocompacted collagen skeleton. *Bioinspir Biomim* 11(3): 036012.

53. Webster, V. A., Chapin, K. J., Hawley, E. L., Patel, J. M., Akkus, O., Chiel, H. J. and Quinn, R. D. (2016b). *Aplysia Californica* as a novel source of material for biohybrid robots and organic machines. In *Biomimetic and Biohybrid Systems* 365-374. Springer International Publishing.

54. WHOI. (2014). HROV *Nereus*. Woods Hole Oceanographic Institute.

55. Wynn, R. B., Huvenne, V. A. I., Le Bas, T. P., Murton, B. J., Connelly, D. P., Bett, B. J., Ruhl, H. A., Morris, K. J., Peakall, J., Parsons, D. R., Sumner, E. J., Darby, S. E., Dorrell, R. M. and Hunt, J. E. (2014). Autonomous underwater vehicles (AUVs): Their past, present and future contributions to the advancement of marine geoscience. *Mar Geol* 352: 451-468.

56. Xu, N. W. and Dabiri, J. O. (2020). Low-power microelectronics embedded in live jellyfish enhance propulsion. *Sci Adv* 6(5): eaaz3194.

57. Xu, N. W., Townsend, J. P., Costello, J. H., Colin, S. P., Gemmell, B. J. and Dabiri, J. O. (2020a). Field testing of biohybrid robotic jellyfish to demonstrate enhanced swimming speeds. *Biomimetics* 5(4): 64.

58. Xu, N. W., Lenczewska, O., Wieten, S. E., Federico, C. A. and Dabiri, J. O. (2020b). Ethics of biohybrid robotic jellyfish modification and invertebrate research. Preprint available on *Preprints*.

59. Yang, G. Z., Bellingham, J., Dupont, P. E., Fischer, P., Floridi, L., Full, R., Jacobstein, N., Kumar, V., McNutt, M., Merrifield, R., Nelson, B. J., Scassellati, B., Taddeo, M., Taylor, R., Veloso, M., Wang, Z. L. and Wood, R. (2018). The grand challenges of Science Robotics. *Sci Robot* 3(14).